JOURNAL OF COMPUTATIONAL PHYSICS 91, 1–21 (1990)

Hairpin Removal in Vortex Interactions*

ALEXANDRE JOEL CHORIN

Department of Mathematics and Lawrence Berkeley Laboratory, University of California, Berkeley, California 94720

Received May 8, 1989; revised September 28, 1989

An algorithm is presented for removing tightly folded hairpins in an evolving collection of vortex filaments. It is argued that this removal provides a model of the effect of the small scales of turbulence. It results in a dynamic smoothing of vortex interactions and in a great reduction in the amount of labor required to sum them. The self-consistency of the model is exhibited numerically. © 1990 Academic Press, Inc.

INTRODUCTION

Recent work [16–18] has shown that turbulence in an incompressible flow can be approximated by a "polymeric" model, which consists of an ensemble of stretched, folded, and pinched vortex tubes. This ensemble resembles in several technical aspects an ensemble of polymers in a solution, at a temperature proportional to the fluid viscosity. It was shown in the earlier calculations and analyses that if the approximating tubes have a cross section of constant circular shape, these tubes must fold if energy is preserved in the vortex stretching process. It has been suggested in the earlier work that the effect of small scales on large scales can be represented by the systematic cancellation and removal of tightly folded "hairpins." As explained below, the tubes are approximating elements and there is no claim that in general all real, physical vortex structures are tubular in shape. A physical vortex is approximated by a cloud of tubular vortices.

The implementation of vortex hairpin removal leads to a rather difficult problem of pattern recognition. The purpose of this paper is to describe a plausible implementation of vortex hairpin removal within the context of a three-dimensional vortex method. The problems that are being addressed are how to recognize a hairpin in a flow represented by a cloud of vortex segments and how to remove it without unduly perturbing the rest of the segments. The solution of these problems will be as simple as we can make it. The resulting algorithm will be applied to the analysis of the motion of a turbulent vortex ring. The numerical results support the belief that the underlying model and its rather crude implementation provide a useful and self-consistent shortcut for the numerical description of turbulence. In particular, three-dimensional vortex methods at high Reynolds number suffer from

* This work was supported in part by the Applied Mathematical Sciences Subprogram of the Office of Energy Research, U.S. Department of Energy, under Contract DE-AC03-76SF000098.

0021-9991/90 $3.00

a catastrophic increase in the number of vortex elements needed to resolve the increasing complexity of the flow, and the present algorithm greatly reduces the problem. It is hoped that similar constructions can be carried out in other contexts; nearby counterrotating structures must appear in any flow where vortex stretching occurs [14, 17], and their cancellation and reconnection should provide a powerful tool for simplifying calculations.

It is worth noting that the vortex algorithm we end up with does not include a vortex core of fixed radius around each vortex segment. Instead, there is smoothing around vortex cores that allows for energy loss and vortex merger. The resulting "blobs" resemble the "blobs" of polymer theory [24, 25] more than the standard blobs of vortex methods. The random walk feature of vortex methods plays a role in the justification of the present model, but not in its implementation, which is entirely deterministic.

We begin by reviewing a vortex method for three-dimensional flow and summarizing the arguments for hairpin removal. The implementation of hairpin removal is then described, and numerical results for the ring problem are presented and discussed. Further work is outlined in the conclusion.

Vortex Methods

Our starting point is the random vortex method, in the general form presented in [13, 23]. More accurate methods that use higher order cores [5, 6] and filaments [2, 30] are available, but will be seen not to be appropriate for use together with the hairpin removal algorithm as we present it.

The Navier–Stokes equations in three space dimensions can be written as

$$\partial_t \xi + (\mathbf{u}\cdot\nabla)\xi - (\xi\cdot\nabla)\mathbf{u} = R^{-1}\Delta\xi \tag{1a}$$

$$\xi = \operatorname{curl}\mathbf{u}, \qquad \operatorname{div}\mathbf{u} = 0, \tag{1b), (1c)}$$

where $\mathbf{u}$ is the velocity, ξ is the vorticity, ∇ is the differentiation vector, $\Delta = \nabla\cdot\nabla$, t is the time, and R is the Reynolds number.

The support of the vorticity ξ is approximated by a union of N "segments" Λ_i, $i = 1, \ldots, N$. Each segment is a circular cylinder of length s_i and radius σ_i. It is characterized by seven numbers: the coordinates $\mathbf{r}_i^b$ of its base, the coordinates $\mathbf{r}_i^t$ of its top ($s_i = |\mathbf{r}_i^t - \mathbf{r}_i^b|$), and σ_i (Fig. 1). Each segment is assumed to be parallel to the vorticity ξ that it carries and is assigned a circulation κ_i equal to the flux of ξ across its cross section. Note that the transformation $\mathbf{r}_i^b \leftrightarrow \mathbf{r}_i^t$, $\kappa_i \to -\kappa_i$ leaves the velocity field produced by the vorticity in Λ_i unchanged. The radius σ is the "cutoff" length. It is assumed that in an appropriate weak sense $\xi \cong \sum \xi_i$, $\xi_i = \xi(\Lambda_i)$. One can imagine the vorticity to be uniformly distributed on Λ_i.

The velocity field due to ξ is

$$\mathbf{u}(\mathbf{r}) = \frac{1}{4\pi}\sum_{i=1}^{N} \kappa_i \frac{\mathbf{a}_i \times \mathbf{s}_i}{\phi(a)},$$

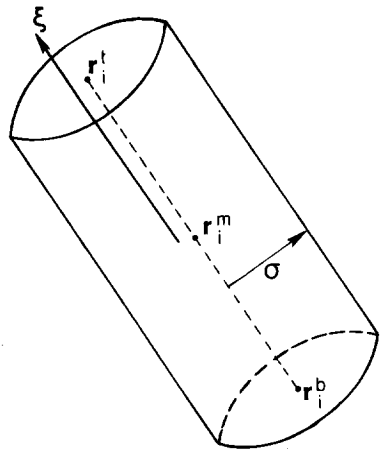

FIG. 1. A vortex segment.

where $\mathbf{s}_i = \mathbf{r}_i^t - \mathbf{r}_i^b$, $\mathbf{a}_i = \mathbf{r} - \mathbf{r}_i^m$, $\mathbf{r}_i^m = \frac{1}{2}(\mathbf{r}_i^t + \mathbf{r}_i^b) =$ center of Λ_i, $a = |\mathbf{a}_i|$, and $\phi(a) = a_i^3$ when $a_i > \sigma_i$, $\phi(a) = \sigma_i^2 a_i$ when $a_i < \sigma_i$. The rule $\phi(a) = a_i^3$ corresponds to the usual Biot–Savart interaction and the modification for $a_i < \sigma_i$ is the smoothing needed for convergence [2, 13], see also below.

The solution of the Navier–Stokes equations can be approximated by the flow described by the stochastic differential equations

$$d\mathbf{r} = \mathbf{u}(\mathbf{r})\, dt + (2/R)^{1/2}\, d\mathbf{w}(t), \tag{2a}$$

$$d\boldsymbol{\xi}(\mathbf{r}) = [(\boldsymbol{\xi} \cdot \nabla)\mathbf{u}]\, dt, \tag{2b}$$

where the quantity in square brackets is evaluated at $\mathbf{r}$ and $\mathbf{w}(t)$ is three-dimensional Brownian motion (see, e.g., [11, 18, 22, 34–36]). We solve Eq. (2) at the top $\mathbf{r}_i^t$ and the bottom $\mathbf{r}_i^b$ of each segment. Vortex stretching is accounted for by the changes in $\mathbf{r}_i^t - \mathbf{r}_i^b$ and no further account has to be taken of Eq. (2b). When $s_i = |\mathbf{r}_i^t - \mathbf{r}_i^b|$ exceeds a predetermined maximum length h, accuracy may be lost and the segment is broken into two halves of equal lengths and cross sections. The new coordinates are obtained by linear interpolation. The stochastic differential equation is solved by a fractional step method, in which the non-random part $d\mathbf{x} = \mathbf{u}\, dt$ is solved by a fourth-order Runge–Kutta method with time step control

$$\Delta t \cdot V \leqslant \tau,$$

where Δt is the time step, $V = \max_i \max_{t,b} |\mathbf{u}(\mathbf{r}_i^{t,b})|$, and τ is a predetermined tolerance. One can readily see that in the absence of random walk and round-off error, this algorithm will preserve the connectivity of a closed vortex tube made up of segments attached end-to-end. Numerical experiment suggests the need for the inequality $\tau \leqslant h$, and we found the choice $\tau = h$ to be satisfactory. We shall never

actually apply the random part of Eq. (2a) in this paper; it is written out for reasons that will appear in the next section.

In this paper, we shall be working in a three-dimensional periodic box of period 1, for the sake of simplicity. Periodicity requires that each vortex segment interact with each other segment and with each one of an infinite array of images of each other vortex. The program is written so that only the largest one of the image interactions is taken into account. In the calculations below all the segments are far enough from the edges of the box so that the interactions are identical to the interactions in a non-periodic unbounded domain. This programming short-cut is mentioned only because the program we shall use is available to any interested reader.

When the method has been used until now, the smoothing parameter σ has been kept constant in each segment, and the same for all segments, see [11, 13]. A smoothing parameter is needed for convergence [2, 5, 11, 19]. The use of a constant σ produces an apparent paradox: it is well known ([45]; see also the analysis in [16, 18]) that the stretching of a vortex tube requires work that is used to spin up the fluid around the reduced cross section. A fixed σ seems to deny this effect. The paradox is only apparent; one should remember that the segments we are using are only computational elements, not physical objects in their own right. A physical vortex will be made up of a cloud of segments; as the cloud stretches its cross section decreases and the spin-up appears. Clearly, a correct handling of this spin-up requires a reasonable numerical resolution, and inasmuch as our goal will be to find a collective representation for coherent portions of a vortex cloud, we may wish to find a more effective, time dependent, core. The other shortcoming of the method we have just described is that in three-space dimensions, at high or infinite Reynolds number R, the L_p norms of the vorticity increase (possibly to infinity in a finite time [14]), and the number of segments required to represent ξ also increases (possibly to infinity in a finite time, see below). We wish to use a theoretical understanding of the stretching process to overcome the need for very large numbers of segments.

One should perhaps restate here a fact that should go without saying: when one approximates a flow by a collection of cylindrical vortex segments, one makes no representation that physical vortices are cylindrical. In fact, vortex approximations have first been used to approximate vortex sheets [19, 20, 31].

Hairpins and Their Removal

We now propose to modify the vortex algorithm just described by (a) allowing the vortex cores to change as the vortex segments stretch, in such a way that volume is conserved and (b) removing vortex "hairpins" as they form. The result of these modifications will be to create a vortex smoothing through a dynamical core.

Step (a) is straightforward: one can assign to each segment an initial cross

section σ_0 (in all the programs below, σ_0 is the same for all segments). It is a matter of easy bookkeeping to decrease σ as the vortices stretch; when a vortex segment is split into two halves because its length exceeds the maximum length h, each half inherits the cross section of its parent. Step (a) is a useful change in the program only when done in conjunction with step (b), the hairpin removal.

Hairpin removal can be explained and justified on several grounds, presented in the order of increasing complexity.

I. A hairpin is a tight U-shaped vortex structure (see Fig. 2). Such hairpins can be seen in numerical calculations (see below). The influence of the vorticity in that hairpin on velocity far away is small, but it reduces the time step needed for accuracy. One can then simply decide to remove it. Such a removal resembles other types of surgery done in vortex calculations, for example [21]. Vortex calculations tend to produce configurations with a lot of details that consume computer time and conceivably add little to the global picture, and one may wish to remove them. The danger, of course, is that their cumulative effect is not negligible.

II. Simplified models [15, 16] and a theory of the inertial range [17, 18] show that hairpins must form in a collection of vortices of circular cross section as they are stretched. The reason is that the energy associated with a straight piece of vortex increases as its radius is decreased, and thus if vortices are stretched while energy is conserved, vortex lines must fold to allow for cancellations between the velocity fields associated with them. The Lamb energy integral [32],

$$T \equiv \frac{1}{2}\int |\mathbf{u}|^2 \, d\mathbf{x} = \frac{1}{8\pi}\int d\mathbf{x} \int d\mathbf{x}' \frac{\boldsymbol{\xi}(\mathbf{x}) \cdot \boldsymbol{\xi}(\mathbf{x}')}{|\mathbf{x} - \mathbf{x}'|}$$

shows that such cancellation can indeed occur, since when $\boldsymbol{\xi}(\mathbf{x}) \cdot \boldsymbol{\xi}(\mathbf{x}') < 0$ the interaction detracts from the total energy. Hairpins thus form, and they form more rapidly if σ is allowed to decrease (for then the energy associated with the vortices increases faster and has to be compensated by folding earlier). The theory and the numerical results in [14, 15, 18] show that the hairpins concentrate on an ever smaller set (in the limit of vanishing viscosity, a set of measure zero), and thus it

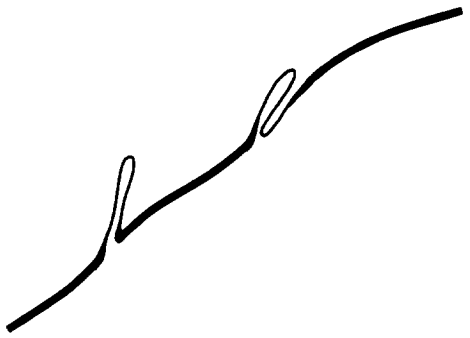

FIG. 2. Hairpins.

is most likely that the cumulative effect of their removal is not large if this removal occurs when they are tight enough.

Furthermore, one cannot rely on the numerical schemes to fold the segment accurately, since accuracy is lost on small enough scales for any finite τ (the parameter that determines the time step). Since one knows that the folding must occur, one can compel neighboring segments to fold tightly as soon as they begin to fold. As is well known from numerical experiment (see, e.g., [9, 14]), if such folding is not enforced, one soon produces spurious chaotic motion on small scales and an unphysical energy increase. The removal of hairpins thus resembles dealiasing in spectral methods [26].

Note that since hairpins must form as a consequence of energy conservation, their removal corresponds to the imposition of energy conservation on small scales by smoothing. This construction is analogous to the way "blobs" impose self-avoidance at small distances in polymer theory [24, 25].

Up to this point, the analysis is made for the segments as computational elements, and no claim is made about the effect of hairpin removal on the physical flow. Presumably this effect must be discovered in each case by actual computation.

III. Abandon now the disclaimer of the preceding paragraph and consider whether hairpin removal cannot be considered as a subgrid model of turbulence. (The possibility that a smoothing of vortex lines could provide such a model was considered earlier in [4, 14].) On moderate scales, not so large that outside stirring interferes, not so small that the core distortion that results from the close proximity of counterrotating vortices can interfere, one can view a turbulent flow as an ensemble of vortex tubes, in thermal equilibrium with a potential background, at a temperature proportional to the viscosity [9, 10, 17, 18]. The random walk term was left in equations (2) to display the analogy with the equations of motion of a polymer in a solvent at a temperature $T \sim R^{-1}$. It is conjectured [17, 18] that such an ensemble has a Kolmogorov-like spectrum, that the tubes behave on moderate scales like self-avoiding walks, and have hairpins on smaller scales that act as energy sinks. Hairpin cancellation is aided by a complex hydrodynamical process that involves a departure from the tube-like structure [3, 29]. Hairpin removal thus models the effect of the small scales on the large scales.

This last rationale for the removal should be viewed with some caution. The turbulence model it is based on is not at present well analyzed. Furthermore, it is not obvious that a turbulence model necessarily leads to a good numerical procedure. For example, in two space dimensions, one can see that isolated vortex patches tend to become circular [10, 12], and if one picks their cores so that the spectrum is $O(k^{-3})$, as in [11], one obtains a vortex method that contains a turbulence model. However, other, physically less well motivated, cores [2, 6] may well provide a better numerical approximation. Nevertheless, this link with turbulence theory will lead to interesting speculations.

Vortex tube models of the dissipation range of turbulence had been proposed in [40, 44]. A tube model related to ours can be found in [8].

IMPLEMENTATION OF HAIRPIN REMOVAL

Suppose we have a collection of N vortex segments Λ_i, $i=1, ..., N$, as in Fig. 1. The length of Λ_i is s_i, its radius is σ_i (σ_i is varying in time), and its cross section is $c_i=\pi\sigma_i^2$. We wish to identify and remove hairpins on vortex lines as well as incipient hairpins, i.e., structures that would have been hairpins if numerical error were absent. This is a difficult problem in pattern recognition, to which the construction below is a plausible but ad hoc solution. Its possible failings are not necessarily a reflection of the incorrectness of the underlying theory.

Consider two segments Λ_i, Λ_j, with bases centered at $\mathbf{r}_i^b$, $\mathbf{r}_j^b$, tops centered at $\mathbf{r}_i^t$, $\mathbf{r}_j^t$, lengths s_i, s_j, cross section $c_i=\pi\sigma_i^2$, $c_j=\pi\sigma_j^2$, and centers $\mathbf{r}_{i,j}^m=\frac{1}{2}(\mathbf{r}_{i,j}^t+\mathbf{r}_{i,j}^b)$ (Fig. 3). The distance between the centers is $r_{ij}=|\mathbf{r}_i^m-\mathbf{r}_j^m|$. We define d_{ij}, the distance between the two segments, to be $d_{ij}=r_{ij}\sin\theta$, where the angle θ is the angle between the segments measured from the segment with the larger cross section, say Λ_i (this choice is dictated by what follows). We pick a maximum distance ρ and consider two segments as being possibly on the same hairpin only if $d_{ij}\leqslant\rho$. Furthermore, they can be on a hairpin only if a folding has started, which will be assumed to have occurred if the inner product of the vorticity in the two segments is negative, $\kappa_i\kappa_j\mathbf{s}_i\cdot\mathbf{s}_j<0$, where $\mathbf{s}_i=\mathbf{r}_i^t-\mathbf{r}_i^b$, etc. The "circulations" κ_i, κ_j must appear in this inner product because of the ambiguity in the representation of the vorticity noted above.

Let q_{ij} be the distance between the centers of the segments projected on the direction of the "fatter" segment Λ_i, $q_{ij}=r_{ij}\cos\theta$. If $\frac{1}{2}(s_i+s_j)\leqslant q_{ij}$ the removal algorithm below will have no consequences, and if $\frac{1}{2}(s_i+s_j)\sim q_{ij}$ the removal algorithm will produce very small segments. We require that possible elements of the same hairpin satisfy the condition $q_{ij}<\beta(s_i+s_j)$, where the parameter β satisfies $\beta<0.5$. The calculation is not sensitive to the value of β, and we generally picked $\beta=0.4$. This constraint says that Λ_i, Λ_j are not far from each other when their distance is measured in their own direction.

Assume that all segments that have undergone little stretching have a location and length that are well approximated by the vortex method; stretching is of course

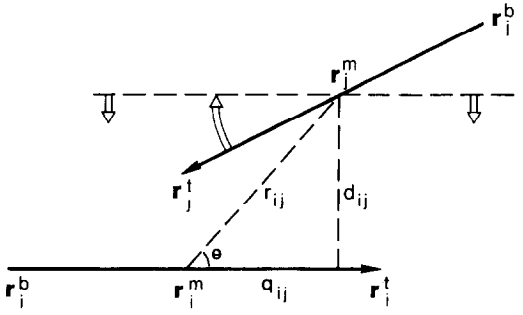

FIG. 3. Relative position of two segments that may be on the same hairpin.

equivalent to decrease in cross section. If little stretching has occurred there is presumably little folding. Assume that initially all the cross sections are equal, and their common value is c_0. Candidates for hairpins to be removed are only those segments for which $c/c_0 \leqslant \alpha$, i.e., those segments that have been stretched at least by a factor $1/\alpha$. Given a segment Λ_j with $c_j/c_0 < \alpha$, we consider those of its neighbors Λ_i whose distance d_{ij} is less than ρ, which satisfy the conditions $\beta(s_i + s_j) > q_{ij}$ and $\kappa_i \kappa_j \mathbf{s}_i \cdot \mathbf{s}_j < 0$. We then consider only the segments that are "fatter" than Λ_j and find among the segments that satisfy all these conditions the one Λ_i that is closest to Λ_j in the sense that d_{ij} is smallest. Of course, there may be no segment that satisfies all these conditions and then no removal involving Λ_j. Λ_i and Λ_j are now assumed to be on the same hairpin and be candidates for partial cancellation when the hairpin is removed. We assume further that the location of the thinner, more stretched segment is less accurately known than that of the fatter segment, and thus one is freer to rotate the thinner segment to achieve cancellation. We thus rotate Λ_j (by construction the thinner of Λ_i and Λ_j) through its center until it is parallel to Λ_i (Fig. 3), with the new direction of Λ_j preserving the negative sign of the inner product of Λ_i and Λ_j. We then bring Λ_i and Λ_j close to each by moving each towards the other along their common normal, each segment moving a distance inversely proportional to its "weight" $s|\kappa|$; i.e., Λ_i moves a distance $d_{ij} s_j |\kappa_j| / (s_i |\kappa_i| + s_j |\kappa_j|)$ and Λ_j moves a distance $d_{ij} s_i |\kappa_i| / (s_i |\kappa_i| + s_j |\kappa_j|)$. The result is two segments that partially overlap. The nonoverlapping pieces are made into new segments, and the overlapping pieces are made into one new segment, with the cross section equal to the sum of the overlapping cross sections, and circulation equal to the sum of the circulation of the overlappings pieces. If the $|\kappa_i|$, $i = 1, \ldots, N$, $N =$ number of segments, are all equal, the segment that results from the overlap will have zero circulation and is thus removable. We shall arrange the approximation at $t = 0$ so that all segments have equal circulation, and thus two segments will give birth to two segments through this process; some of the new segments may be very short. For the possible configurations of the cancelling segments, see Fig. 4.

FIG. 4. Cancelling vorticity in hairpins.

Note that only one of the segments is rotated. One can think of more elaborate rotation schemes in which both segments turn. We have not yet found a more elaborate scheme that seems to improve on the results below.

The over-all process runs as follows: one starts with the segment Λ_j that has the smallest c_j/c_0. One looks for a neighbor to pair it with; if there is one, the pairing and removal are done. If there is no suitable neighbor, one goes on to the next segment with a larger or equal c_j/c_0. A piece of a segment may be paired more than once; i.e., it is possible for a segment to be paired to another one, and then for one of the surviving pieces to be paired once again. The process stops when one reaches a segment Λ_j with $c_j/c_0 \geqslant \alpha$. A running record of the last value of c_j/c_0 reduces the amount of searching needed. Any segment for which $s\,|\kappa| < s_{\min}$ is removed (so that in particular segments with $\kappa = 0$ are removed). We picked $s_{\min} = 0.001$; this value is so conservative that it has no impact on the outcome of the calculation and could safely be raised. The removal is done once every time step.

The remaining numerical parameters are: β, α, ρ. β will be left at the fixed value $\beta = 0.4$. Clearly, the larger ρ or α the more cancellation will occur, and when we are testing the effect of the removal we are able to vary either. We conjecture that the important parameter is a product of the form $\rho^g\alpha$, where $g > 0$ depends on the vorticity dimension D [14, 15], but we fix ρ at the plausible value $\rho = h$ (the maximum segment length) and present numerical results obtained with different values of α; α thus determines the onset of hairpin removal.

The Motion of Vortex Rings

We apply the algorithm just described (a vortex method with hairpin removal) to the motion of a thin circular vortex ring with unit circulation. The ring is characterized by the radius A of its axis and the radius q of its cross section (Fig. 5). There are no solid boundaries in this problem, and thus the random walk part of Eq. (2)

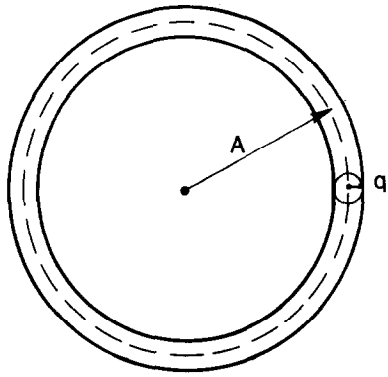

FIG. 5. A vortex ring.

can be omitted. The physical vortex ring is approximated initially by N filaments made up of segments attached end-to-end; the circulation is divided evenly among them. One of these filaments coincides with the axis of the cylinder, and $(N-1)$ are distributed around it on a circle of radius q. A detailed application of a vortex method to this problem, together with stability results and a parameter study, can be found in [30]; related problems have been considered in [4, 14].

The velocity of the ring is given by [32]

$$U = (\log(8A/q) - C)/4\pi A,$$

where the constant C depends on the distribution of the vorticity in the ring and is thus dependent on the number of filaments. Furthermore, the radius q is poorly defined in the numerical approximation. For a constant distribution of vorticity in the ring $C = 0.25$, we present calculations for which $A = 0.18$ and $q = 0.05$. The value of U that corresponds to these parameter values in the formula above is $U = 1.375$, but an error of about 10% can be expected as a result of the uncertainty in the way the radius q is imposed and of the non-constancy of the vorticity distribution in the numerical model.

The stability of this type of vortex ring has been analyzed exhaustively [39, 46]. In Fig. 6 we present a calculation in which the ring is represented by these filaments, with a fixed segment radius $\sigma = 0.1$, τ, the parameter that determines the time step in the Runge–Kutta integration, equal to 0.05, and h = maximum segment length = τ. More extensive calculations along these lines can be found in [30]. The only perturbations that exist in the flow are due to round-off errors; a relatively large value of σ has been picked to delay the onset of instability. The calculation starts with $N = 72$ segments and proceeds until $N = 600$. The most unstable mode has 12 nodes, corresponding faithfully to the most unstable wave number. A careful comparison between numerical results and stability theory is also available in [30]. Note that hairpins form but there is little folding in the direction of the axis; the perturbation due to round-off is not sufficient to break the radial symmetry of the problem before N becomes relatively large. The introduction of a variable σ and the removal of the hairpins have a minimal effect on this calculation. The conclusion is that a vortex method is able to display the initial instability but becomes expensive rapidly; hairpin removal does not affect this conclusion to a significant extent; some form of turbulence is necessary to exhibit its power.

There is a substantial experimental literature on turbulent vortex rings [37, 38]. The statistically steady vortex rings that have been observed consist of a rapidly rotating coherent narrow core that exchanges vorticity with a wider region with weak vorticity, into which outside fluid is entrained and is then expelled downstream. Such rings are created by expelling a fluid slug from an orifice, and their modelling is beyond the scope of the present paper. The dynamics of a ring depend on the initial conditions, and we know of no experiment that corresponds to initial conditions that consist of a coherent ring surrounded by potential flow.

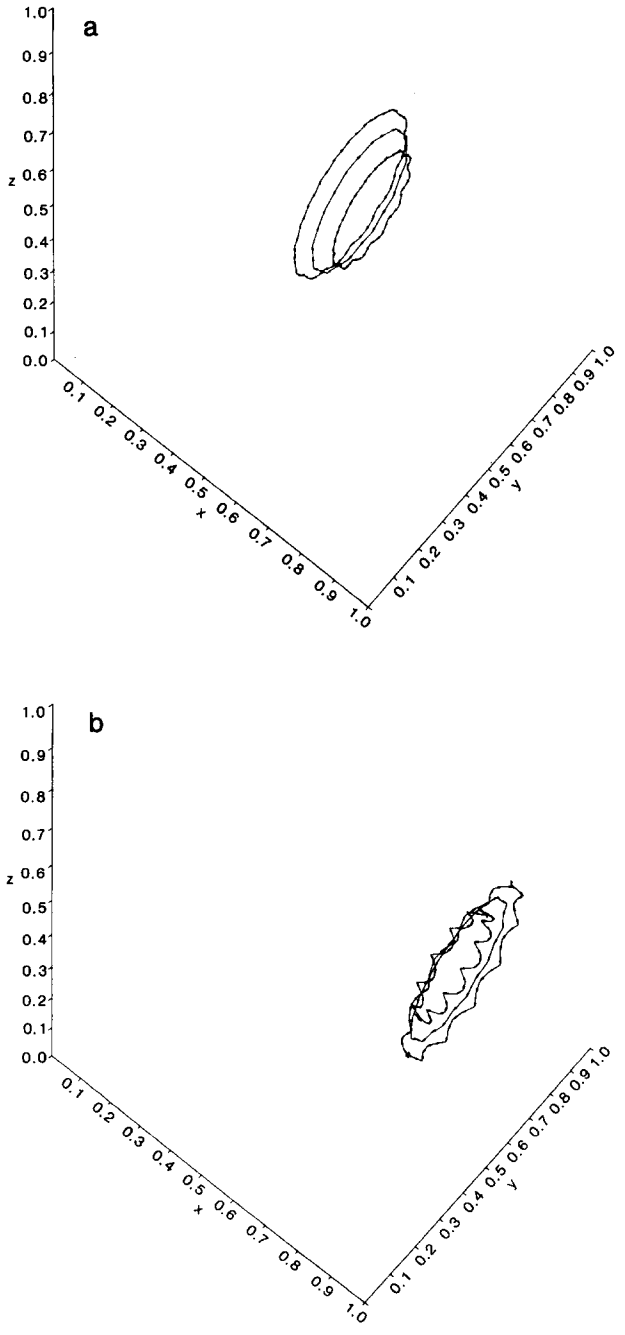

FIG. 6. Instability of a vortex ring: (a) initial conditions; (b) $t = 0.15$; (c) $t = 0.30$; (c) $t = 0.40$.

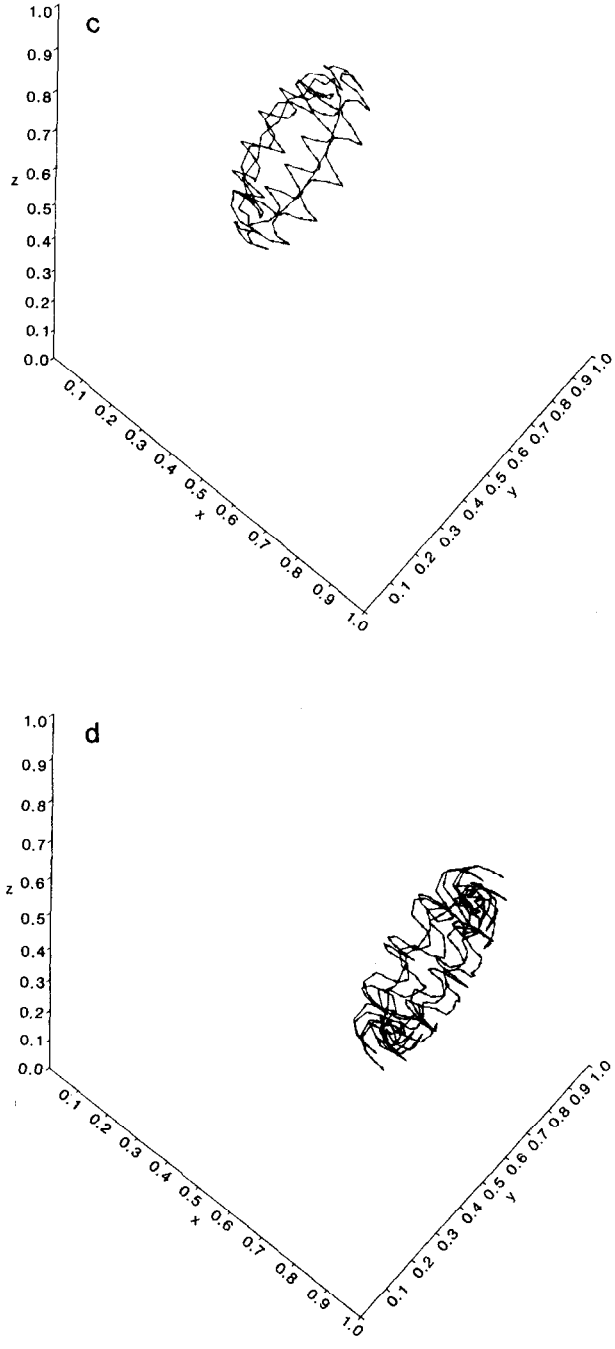

FIG. 6—*Continued*

The following experimental observations will be useful to the interpretation of the results below: (a) vortex rings slow down, (b) as mentioned above, stable vortex rings consist of a coherent core surrounded by a vortical cloud, (c) the quantity $dA/d\bar{x}$ is of order 10^{-2}, where A is the radius of the axis of the ring and $\bar{x}$ is the distance travelled by the ring, (d) solitary waves stabilize the ring, (e) the behavior of the ring is a sensitive function of initial conditions, of the ambient flow, and of a hard to quantify degree of organization of the ring.

In order to obtain a ring that can be viewed as "turbulent" we perturb the initial data by giving one point on the center filament a perturbation of amplitude 10^{-2}. This results in solitary waves moving on the ring [14, 33] and leads to a break in the symmetry of the ring that allows axial folding to occur. Presumably, this folding and the resulting formation of removable hairpins is a form of stabilization. The ring thickens, and this thickening may be viewed as a stage in the formation of a surrounding vortical cloud. The ring eventually collapses; this collapse follows an apparent singularity formation (see the next section for details). Such collapse is not seen in the experimental data quoted, which, of course, relate to different initial and boundary conditions, but it does appear in casual observations of smoke rings subject to disturbances from the ambient fluid. The numerical observations are described in detail in the next section. Note that structures that persist yet entrain and expel fluid have been observed in other vortex calculations [41].

Numerical Results

Our major numerical results are summarized in Fig. 7 and 9, which show that with vortex hairpin removal one obtains a self-consistent approximation that keeps the computational effort within acceptable bounds.

The calculations are started with three vortex filaments, one of which is perturbed. $\sigma = 0.05$ initially for all segments, $N =$ number of segments $= 72$. The other numerical parameters are $h = \tau = \rho = 0.05$; we have carefully checked that these choices provide an adequate resolution and that further refinement does not change the conclusions. The remaining parameter is α; $1/\alpha$ is the amount of stretching a segment has to undergo before it becomes a candidate for inclusion in a removable piece of hairpin. The calculation was stopped whenever the number of segments exceeded 800; if $\alpha \leqslant 0.025$, this limit was exceeded before any hairpin removal had occurred; thus $\alpha = 0.025$ and $\alpha = 0$ are indistinguishable.

In Fig. 7 we plot the number N of vortex segments as a function of time for $\alpha = 0.15$, $\alpha = 0.05$, and $\alpha \leqslant 0.025$. Clearly the number of segments increases as α decreases. For $\alpha \leqslant 0.025$ it quickly becomes intolerable. Since N is roughly proportional to the L_1 norm of the vorticity, this graph suggests that the solution of Euler's equation for this ring problem blows up around $t = 0.18$–0.19. Clearly, vortex hairpin removal reduces the amount of labor in the calculation. In Fig. 8 we plot the time step Δt as a function of t (as restricted by $\Delta t \cdot U \leqslant \tau$) for $\alpha = 0.05$ and

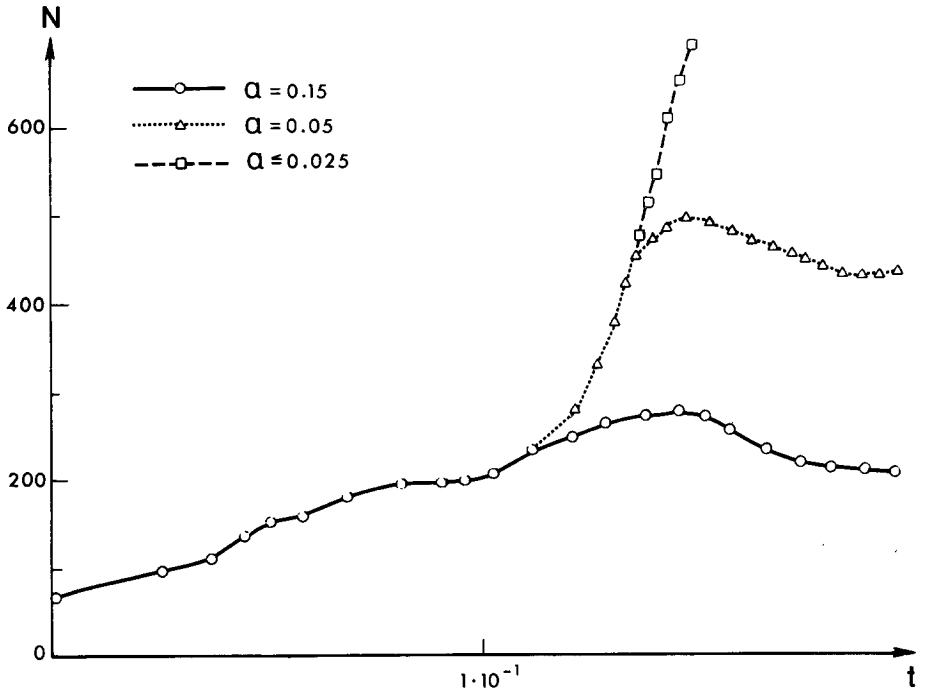

FIG. 7. Number of segments N as a function of t.

$\alpha \leqslant 0.025$. Clearly, Δt decreases as α decreases, thus further increasing the amount of labor required to find the evolution of the ring as a function of t. With $\alpha \leqslant 0.025$ the calculation cannot be continued with $N \leqslant 800$ for $t > 0.155$. The removal of hairpins thus accelerates the calculation by a huge factor. The remaining question is whether the numerical results are trustworthy. At present the answer to this question cannot be absolute. Some indications can be found from the study of the ring.

In Fig. 9 we plot the velocity of the ring U as a function of t. U is calculated as follows: the axis of the ring is set initially in a plane parallel to the (y, z) plane, and the x coordinate x_c^n of the center of the ring after n steps is calculated by the formula

$$x_c^n = \frac{\sum x_i^m w_i}{\sum w_i},$$

where x_i^m is the x-coordinate of the center of the ith segment after n steps and the weight w_i is $w_i = |\kappa_i| s_i$. At the time t that corresponds to n steps, the velocity is calculated as $U(t) = (x_c^n - x_c^{n-1})/\Delta t$.

After the first few steps the velocity U is highly oscillatory and oscillates more for smaller values of α. We ascribe this oscillation to the effect of the hairpins, which give large local curvatures and thus rotate rapidly. To obtain a readily intelligible

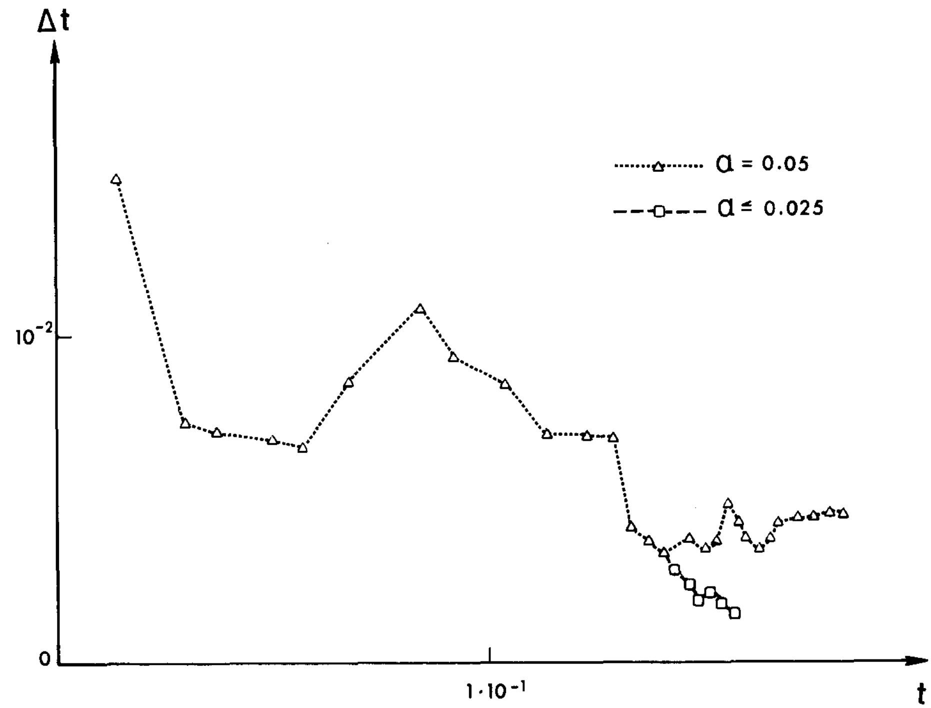

FIG. 8. Time step Δt as a function of t.

graph, after the first five steps we replace the local $U(t)$ by the average of the last five values of U. Since Δt is not fixed and not independent of α, this averaging has a slight distorting effect on the comparisons below.

In Fig. 9 we plot the functions $U(t)$ so obtained for several values of α. For $\alpha > 0.15$ the graph begins to flatten substantially, and thus values with $\alpha > 0.15$ are too large. For $\alpha < 0.05$ the graphs coincide to the extent that they can be traced with $N \leqslant 800$. The slight discrepancy between $\alpha = 0.05$ and $\alpha \leqslant 0.025$ during the short time where the latter is both computable and different from the former can be ascribed to the effect of the time averaging. The difference between $\alpha = 0.15$ and [illegible] between $t = 0.1$ and $t = 0.2$. It is tempting to ascribe this difference to the presence of a large hairpin that is removed in one case and not the other. Already in [14] we saw a large fluctuation in various averaged quantities that coincided with the appearance of a large hairpin (but a cause to effect relationship has not been established).

The most interesting feature of Fig. 9 is the "crisis" around $t = 0.2$, during which the velocity drops nearly to zero. The timing of this "crisis" depends on the initial perturbation. A qualitatively similar crisis appears in the graph of the kinetic energy as a function of time; this graph is not reproduced because its accuracy is very

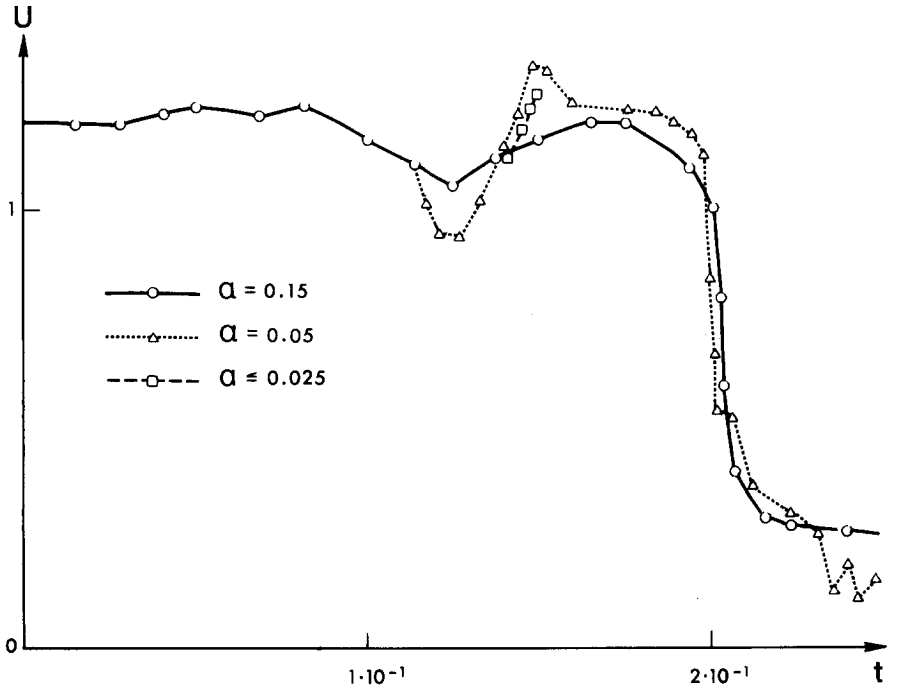

FIG. 9. Ring velocity U as a function of t for the perturbed ring.

suspect: as discussed in [14], it is very difficult to evaluate the kinetic energy accurately for a highly intermittent vortical flow. The onset of the "crisis" follows the estimated time of singularity formation, and it is tempting to believe that the two are related. A similar observation has been made recently in a difference calculation [7], and qualitatively similar observations have been made in the problem of sheet motion in the plane [31], where a singularity also appears.

One can try to check the calculation by checking the constancy of certain invariants. The three components of the integral $\int \xi \, d\mathbf{x}$ should be zero for a collection of closed vortex lines, and a verification of this fact checks that the representation of the lines by disconnected segments and the rotation in the merger process are not harmful. The dangers are greatest for the larger values of α. In the worst case we have presented, $\alpha = 0.15$, the components of the normalized quantity $\int \xi \, d\mathbf{x} / \int |\xi| \, d\mathbf{x}$ oscillate slightly around 0, the largest value in the interval of interest $0 \leqslant t \leqslant 2$ being 0.03. If one keeps on running for a longer time the oscillation can become larger (a value of 0.13 has been observed at $t = 3.5$ with $\alpha = 0.15$), but these values are consistent with the growth of truncation error in a thermalized environment. Other invariants of smooth inviscid flow, for example the impulse, cannot be expected to remain constant (and in fact could not be constant if the energy and

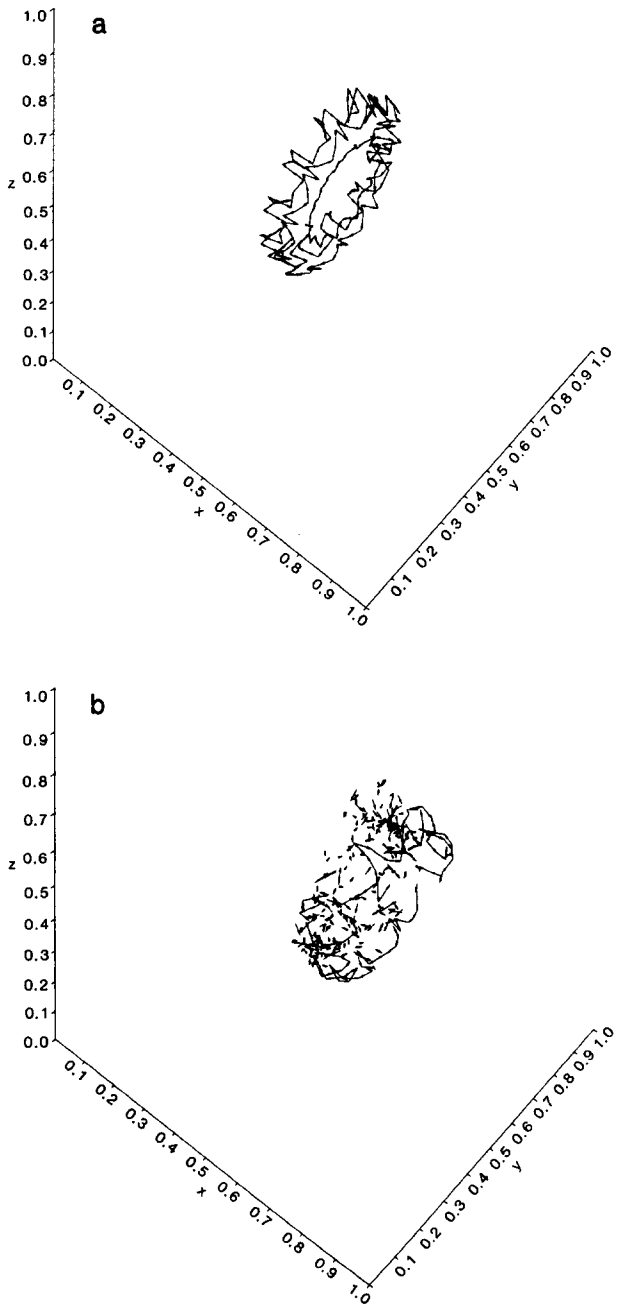

FIG. 10. Vortex configuration for the perturbed ring ($\alpha = 0.075$): (a) $t = 0.11$; (b) $t = 0.16$; (c) $t = 0.21$; (d) $t = 0.40$.

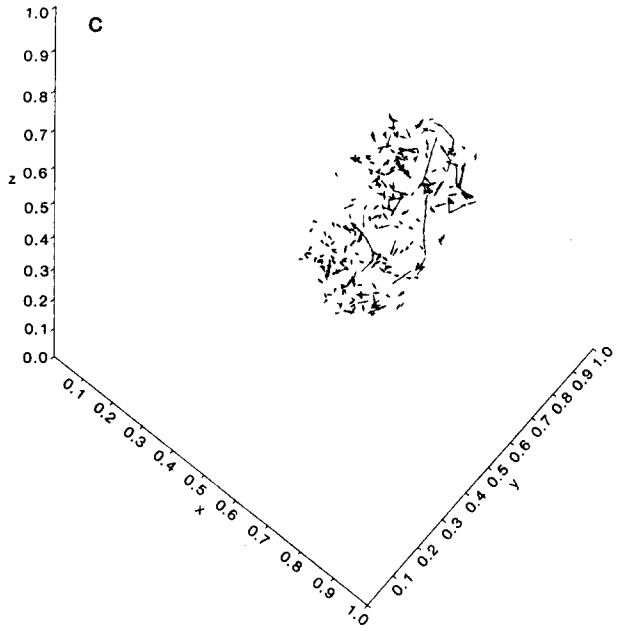

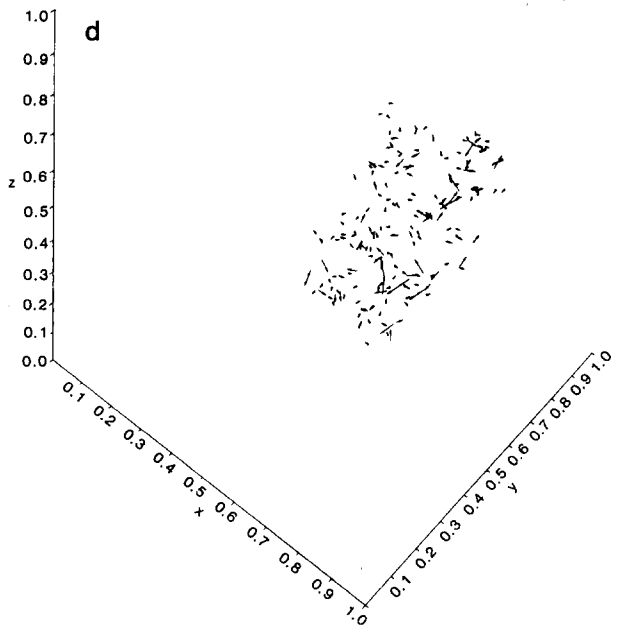

FIGURE 10—*Continued*

U decrease). This is no cause for alarm. Folded vortex regions shoot off and carry impulses away from the central flow region and their removal decreases the total impulse, in our implementation or any other. This removal should not affect the organized part of the flow.

The radius A of the vortex ring changes in time; a numerical approximation to it is

$$A^2 = \sum_i ((y_i^m)^2 + (z_i^m)^2)_i \, w_i \Big/ \sum w_i.$$

with $\mathbf{x}_i^m = (x_i^m, y_i^m, z_i^m)$ and $w_i = |\kappa_i| s_i$ as before. A increases in time, with computed value of $dA/d\bar{x}$, $x =$ distance travelled, of order ~ 0.01–0.02, comparable to the experimental values in the nearly steady vortex experiments. The experimental and the numerical conditions are quite dissimilar, so it is unclear what significance should be attached to this observation.

In Fig. 10 we display a visualization of the flow at various times. Hairpins appear and the flow eventually becomes disorganized. The only surprise in these pictures is that casual observation leads to misleading conclusions about the flow. At time $t = 0.16$ the flow appears quite disorganized, yet U, the velocity of the ring, is still at its "organized" value before the crisis. Better visualization techniques remain to be discovered (see the discussion in [42]).

The program as we have written it is logic-intensive, since the search for possible hairpins has not been optimized. Bin-partition schemes, such as the ones used in conjunction with fast vortex summations [1, 27], would improve the program's efficiency. A typical run with $\alpha = 0.1$ takes about 3 h on a Sun 2 work station or 15 min on a Cray 1; most of the time is spent in locating hairpins.

Conclusions and Speculations

The main conclusion from the calculation is that vortex hairpin removal is a reasonable way of simplifying vortex calculations. The next steps should be to apply it to more complicated problems and to marry it with fast summation algorithms, both in order to speed the vortex summation part and to simplify the search for hairpins.

There is no reason why vortex hairpins cannot be recognized and detected in a calculation based on finite differences or on a spectral representation. The problem of identifying hairpins is probably harder in these other contexts but not necessarily insurmountable.

If one interprets the removal of hairpins as the mechanism of energy loss in a turbulent medium, then the calculations above lead to interesting speculations. Hairpin removal creates regions of high vorticity that are not connected (i.e., vortex tubes that are alternately very thin and quite fat), as can be seen in Fig. 9. The

pictures obtained by spectral methods (see, e.g., [43, 47]) are quite similar, and suggest that an unrecognized process of hairpin cancellation occurs there too.

In the spectral calculation in [47] it was observed that much of the energy dissipation occurs elsewhere than where the absolute value of the vorticity is large. Assuming that this observation is not due to numerical dissipation, one can conjecture that hairpin cancellations are still going on in regions where the vorticity amplitude has already decayed and, in fact, that this is how the disconnected high $|\xi|$ regions are formed. (The surprising conclusions of [47] were pointed out to me by R. Kraichnan.)

More generally, the calculations above provide supporting evidence for the belief that hairpins play a major role in the mechanics of turbulence (as was suggested in [15, 16, 30], and as is already quite firmly known to be the case near walls [28]) and also provide supporting evidence for the usefulness of polymeric models.

Note. The program used above is available from the author.

REFERENCES

1. C. ANDERSON, *J. Comput. Phys.* **62**, 111 (1986).
2. C. ANDERSON AND C. GREENGARD, *SIAM J. Numer. Anal.* **22**, 413 (1985).
3. C. ANDERSON AND C. GREENGARD, *Commun. Pure Appl. Math.* **42**, 1123 (1989).
4. S. BALLARD, Parametrization of viscosity in three dimensional vortex methods, in *Numerical Methods in Fluid Mechanics*, edited by K. Morton and J. Baines (Clarendon, Oxford, 1986).
5. J. T. BEALE AND A. MAJDA, *Math. Comput.* **39**, 1 (1982).
6. J. T. BEALE AND A. MAJDA, *J. Comput. Phys.* **58**, 188 (1985).
7. J. BELL, Applied Mathematics Group, Lawrence Livermore National Laboratory, Livermore, CA, private communication (1988).
8. S. CHILDRESS, *Geophys. Astrophys. Fluid Mech.* **29**, 29 (1984).
9. A. J. CHORIN, Report NYO-1480-135, Courant Institute, New York University, 1969 (unpublished).
10. A. J. CHORIN, in *Proceedings, 2nd Int. Conf. Numer. Methods Fluid Mech.* (Springer-Verlag, New York, 1970).
11. A. J. CHORIN, *J. Fluid Mech.* **57**, 785 (1973).
12. A. J. CHORIN, *J. Fluid Mech.* **63**, 21 (1974).
13. A. J. CHORIN, *SIAM J. Sci. Stat. Comput.* **1**, 1 (1980).
14. A. J. CHORIN, *Commun. Math. Phys.* **83**, 517 (1982).
15. A. J. CHORIN, *Commun. Pure Appl. Math.* **39** (special issue), S47 (1986).
16. A. J. CHORIN, *Commun. Math. Phys.* **114**, 167 (1988).
17. A. J. CHORIN, *Phys. Rev. Lett.* **60**, 1947 (1988).
18. A. J. CHORIN, in *Vortex Methods*, edited by K. Gustafson and J. Sethian (SIAM, Philadelphia, 1989).
19. A. J. CHORIN AND P. BERNARD, *J. Comput. Phys.* **13**, 423 (1973).
20. R. CLEMENTS AND D. MAULL, *Prog. Aeronaut. Sci.* **16**, 129 (1975).
21. D. DRITSCHEL, *J. Comput. Phys.* **77**, 240 (1988).
22. R. ESPOSITO AND M. PULVIRENTI, Three dimensional stochastic vortex flows, preprint, Rome University, 1987 (unpublished).
23. D. FISHELOV, *SIAM J. Sci. Stat. Comput.* **11**, 399 (1990).
24. K. FREED, *Renormalization Group Theory for Macromolecules* (Wiley, New York, 1987).
25. P. G. DE GENNES, *Scaling Concepts in Polymer Physics* (Cornell Univ. Press, New York, 1971).

26. D. GOTTLIEB AND S. ORSZAG, *Numerical Analysis of Spectral Methods* (SIAM, Philadelphia, 1977).
27. L. GREENGARD AND V. ROKHLIN, *J. Comput. Phys.* **73**, 325 (1987).
28. M. HEAD AND P. BANDYOPADHYAY, *J. Fluid Mech.* **107**, 297 (1981).
29. R. KERR, "Simulation of Vortex Reconnection," manuscript, Physics Department, Cornell University, 1988 (unpublished).
30. O. KNIO AND A. GHONIEM, *J. Comput. Phys.* **86**, 75 (1990).
31. R. KRASNY, *J. Comput. Phys.* **65**, 292 (1986).
32. H. LAMB, *Hydrodynamics* (Dover, New York, 1932).
33. S. LEIBOVICH AND J. RANDALL, *J. Fluid Mech.* **51**, 625 (1972).
34. A. LEONARD, *Annu. Rev. Fluid Mech.* **17**, 523 (1985).
35. D. G. LONG, *Math. Comput.*, in press.
36. A. MAJDA, "The Mathematical Foundations of Incompressible Flow," lecture notes, Princeton, 1986.
38. T. MAXWORTHY, *J. Fluid Mech.* **81**, 465 (1977).
39. P. SAFFMAN, *J. Fluid Mech.* **84**, 625 (1978).
40. P. SAFFMAN, in *Topics in Nonlinear Physics*, edited by N. Zabusky (Springer-Verlag, New York, 1968).
41. J. SETHIAN AND A. GHONIEM, *J. Comput. Phys.* **74**, 283 (1988).
42. J. SETHIAN, J. SALEM, AND A. GHONIEM, in *Proceedings, Supercomputing 88*, (IEEE, New York, 1988).
43. E. SIGGIA, *J. Fluid Mech.* **107**, 375 (1981).
44. H. TENNEKES, *Phys. Fluids* **11**, 669 (1968).
45. H. TENNEKES AND J. LUMLEY, *A First Course in Turbulence* (MIT Press, Cambridge, 1972), p. 257.
46. S. WIDNALL, *Annu. Rev. Fluid Mech.* **8**, 141 (1976).
47. K. YAMAMOTO AND I. HOSOKAWA, *J. Phys. Soc. Japan* **57**, 1532 (1988).